

Local dark energy in the Sculptor Filament of galaxies

M. V. Pruzhinskaya^{1,*} • A. D. Chernin¹ •
I. D. Karachentsev²

Abstract Two dozens of different mass galaxies observed at distances less than 10 Mpc from the Local Group are organized in the elongated structure known as the Sculptor Filament. We use recent Hubble Space Telescope data on local galaxies to study the dynamical structure and evolutionary trends of the filament. An N-body computer model, which reproduces its observed kinematics, is constructed under the assumption that the filament is embedded in the universal dark energy background. In the model, the motions of the filament members are controlled by their mutual gravity attraction force and the anti-gravity repulsion force produced by the local dark energy. It is found that the dark energy repulsion dominates the force field of the outer parts of the filament. Because of this, the filament expands and its expansion proceeds with acceleration. The dark energy domination increases with cosmic time and introduces to the filament the linear velocity–distance relation with the universal time-rate (“the Hubble constant”) that depends asymptotically on the dark energy density only.

Keywords galaxies: groups: general – galaxies: kinematics and dynamics – dark energy

1 Introduction

The studies of the cosmic kinematics and dynamics started in the 1910s when Slipher discovered the recess-

sion motions of nearby galaxies. In 1922–24, Friedmann published his now famous theory of the uniform universe. According to the theory, the universe as a whole is not static, it is expanding, and its expansion motion follows the linear velocity–distance relation. The same linear relation known as the “Hubble-Lemaître Law” was found by Lemaître in 1927 (Lemaître 1927), Robertson in 1928 (Robertson 1928), and Hubble in 1929 (Hubble 1929) in the observed motions of local (distances of ~ 1 –30 Mpc) galaxies. Is there any fundamental interconnection among the local motions of galaxies with the global expansion motion of the Universe as a whole? The question has been opened for decades.

Friedmann’s global theory assumes that the matter distribution is uniform in the global universe. The real universe is uniform indeed, but this is the uniformity in average over the global space scales of ~ 1000 Mpc and larger. This fact has been confirmed rather recently, in 1990s, by observations with the Hubble Space Telescope and other modern astronomical instruments. As for the local space, the matter distribution is highly non-uniform there: the nearby galaxies are mostly collected in the building systems of the Cosmic Web which are groups, clusters, superclusters (“Zeldovich pancakes”), filaments of galaxies. Friedmann’s theory is not applicable there; this theory cannot predict, explain or describe the local astronomical findings of the 1920s. The observed motions on both local and global space scales can be similar, only if they are all essentially controlled by a common strong physical factor. This factor really exists: it is dark energy.

The solution to the long-standing problem (Chernin et al. 2010) was suggested soon after the discovery of dark energy at the global cosmological distances (Riess et al. 1998; Perlmutter et al. 1999). The solution is based on the following arguments: the astronomers (Riess et al. 1998; Perlmutter et al. 1999)

M. V. Pruzhinskaya

A. D. Chernin

*Corresponding author, pruzhinskaya@gmail.com

Lomonosov Moscow State University, Sternberg Astronomical Institute, Universitetsky pr. 13, Moscow, 119234, Russia

I. D. Karachentsev

Special Astrophysical Observatory RAS, Nizhnij Arhyz, 369167, Russia

found dark energy indeed; dark energy is described by Friedmann’s theory with Einstein’s cosmological constant; on the local space scales (1–30 Mpc), the anti-gravity of dark energy is as strong as the gravity produced by the matter of galaxies there. The first two (“global”) arguments are confirmed by all the development of cosmology for the last two decades. As for the third (“local”) argument, it includes dark energy to the local dynamics of galaxies in a natural way because Einstein’s cosmological constant is constant and so dark energy has the same density on both global and local scales¹. This argument is supported by a set of computer models developed for really existing systems of galaxies embedded in the dark energy omnipresent background. These systems are as following: the Local Group (LG) of galaxies together with the expansion outflow of dwarf galaxies around it, several systems similar to the Local Group, two clusters of galaxies (Coma and Virgo) with their expansion outflows, the Local Supercluster of galaxies, or “Zeldovich pancake” (see Chernin 2001, 2008, 2013; Chernin et al. 2015, and references therein).

The set of the models is not complete. Indeed, the three types of galaxy systems are known as the basic building blocks of the observed Cosmic Web. They are the three-dimensional (3D) groups and clusters, two-dimensional (2D) walls like the Local Supercluster and one-dimensional (1D) filaments. In our set of the local models, 3D and 2D systems are represented and there is no 1D systems which are very typical elements of the large-scale structure (Tempel et al. 2014). To fill this lack, a Λ N-body model is suggested in the present work. This is the model of the nearby Sculptor Filament of galaxies, a loose filament of galaxies located in the immediate proximity of the Local Group (see Sec. 3). The filament is an expanding system, and it will be shown below that anti-gravity of dark energy plays an important role in its dynamics. Because of this, the expansion of the system proceeds with acceleration approaching with time the linear velocity-distance relation.

The basic astronomical data for the theory are provided by the Hubble Space Telescope (HST) observations (Karachentsev et al. 2003, 2013).

Note that more than half a century ago, de Vaucouleurs (1959) described the Sculptor Filament as an “expanding association of galaxies” which “has a total positive energy “being” of the type predicted by Ambartsumian”. Now one may see that the physical nature

of the filament expansion is rather due to omnipresent dark energy (which is hardly less mysterious than the “superdense D-bodies”², but nevertheless really existing in Nature).

2 Dark energy on local scales

According to the concept suggested by Gliner (1966), dark energy may be treated topically as a vacuum-like continuous medium. This medium cannot serve as a reference frame, since it is comoving to any matter motion — similarly to trivial emptiness. Its density is perfectly uniform, the same in any point of the space and any moment of time. The dark energy density is given by Einstein’s cosmological constant:

$$\rho_\Lambda = \Lambda/(8\pi G), \quad (1)$$

where G is the Newtonian gravitational constant; the speed of light $c = 1$ here. Dark energy density ρ_Λ is positive and its currently adopted value $\rho_\Lambda \simeq 0.7 \times 10^{-29}$ g/cm³ (Riess et al. 1998; Perlmutter et al. 1999; Scolnic et al. 2018). The dark energy equation of state is

$$p_\Lambda = -\rho_\Lambda. \quad (2)$$

Here p_Λ is the dark energy pressure which is negative, while its density is positive.

General Relativity (GR) indicates that the “effective gravitating density” of any medium is determined by both density and pressure of the medium:

$$\rho_{eff} = \rho + 3p. \quad (3)$$

The effective density of dark energy,

$$\rho_\Lambda + 3p_\Lambda = -2\rho_\Lambda < 0, \quad (4)$$

is negative, and it is because of this sign “minus” that dark energy produces not attraction, but repulsion, or anti-gravity.

A simple example of the GR exact solution with non-zero dark energy is the Schwarzschild-de Sitter space-time which gives the metric outside a spherical matter mass M embedded in the dark energy of the constant density ρ_Λ :

$$ds^2 = Y dt^2 - R^2 d\Omega^2 - Y^{-1} dR^2. \quad (5)$$

¹The tension between the global and local H_0 measurements (Planck Collaboration et al. 2018; Riess et al. 2019) can be due to some unknown systematics and not necessary includes the additional physics beyond the current standard cosmological model and discussed in Freedman et al. (2019).

²One of the concepts of the formation of stars and galaxies existed in 1960–1970s. In particular, according to this concept clusters of galaxies arise from a number of explosions of superdense protostellar objects, D-bodies (Ambartsumian 1958a,b; Ambartsumyan 1962; see also Chernin 1971).

Here R is the distance from the center of the mass, $d\Omega^2 = \sin^2 \theta d\phi^2 + d\theta^2$ and

$$Y(R) = 1 - 2\frac{GM}{R} - \frac{8\pi}{3}\rho_\Lambda R^2. \quad (6)$$

The metric of equations (5, 6) is static, contrary to Friedmann's time-dependent spacetime. As it is seen from equation (6), the gravity of the mass M becomes negligible in comparison with the dark energy anti-gravity, at infinitely large distances. In this space limit, the metric tends to de Sitter's metric which is determined by dark energy only:

$$Y(R) \simeq 1 - \frac{8\pi}{3}\rho_\Lambda R^2, \quad R \rightarrow \infty. \quad (7)$$

It is remarkable that Friedmann's cosmological metric with dark energy has the same de Sitter static asymptotic at infinitely large time in standard cosmology.

In the Newtonian terms, equations (5, 6) describe the gravity-anti-gravity force field, where Newtonian gravity is produced by the mass M and Einstein's anti-gravity is produced by dark energy. If the force field is weak, so that deviations from the Galilean metric are small, the metric of equation (7) may be reduced to the Newtonian description in terms of the gravity-antigravity potential U :

$$Y^{1/2} \simeq 1 + U, \quad U(R) = -\frac{GM}{R} - \frac{4\pi G}{3}\rho_\Lambda R^2. \quad (8)$$

In this approximation, the force (per unit mass) comes from equation (8):

$$F(R) = -\frac{dU}{dR} = -\frac{GM}{R^2} + \frac{8\pi G}{3}\rho_\Lambda R. \quad (9)$$

In the rhs here the sum of the Newtonian force of gravity and Einstein's force of anti-gravity are given for unit mass, i.e. acceleration.

It is seen from equation (9) that gravity may dominate at small distances from the mass M , while anti-gravity may be stronger than gravity at large distances. Gravity and antigravity balance at the distance

$$R = R_\Lambda = \left(\frac{M}{\frac{8\pi}{3}\rho_\Lambda} \right)^{1/3}. \quad (10)$$

The radius R_Λ is the radius of the “zero-gravity sphere” (Chernin 2001, 2016). It appears here as the local spatial counterpart of the “zero-gravity moment” in the global expansion of the Universe which occurred at the cosmic redshift 0.7 about 7 Gyr ago.

The Newtonian approximation of equations (7–10) is appropriate for local systems, since the velocities of the expansion flows are very small compared to the

speed of light, and the spatial differences in the gravity-antigravity potential are very small compared to the speed of light squared there. This approximation was used in the 3D and 2D models of the Cosmic Web systems (see Chernin 2001, 2008; Chernin et al. 2015, and references therein). It is also used below for the 1D model of the Sculptor Filament of galaxies.

3 Sculptor Filament: 1D local expansion flow

The closest to the Local Group the association of the bright galaxies (NGC0055, NGC0247, NGC0253, NGC0300, and NGC7793) including a number of dwarf galaxies is known as the Sculptor group. However, it turns out that the Sculptor group does not constitute a single, compact, gravitationally-bound group, but rather to be a loose filament of galaxies of 1×6 in size extended along a line of sight over ~ 5 Mpc (Arp 1985; Jerjen et al. 1998; Karachentsev et al. 2003, 2004). Following Westmeier et al. (2017) we use the term “Sculptor Filament” for it throughout this paper. In fact, the Local Group forms a part of this filament (Karachentsev et al. 2003). Due to our location within the Sculptor Filament, we see the sub-groups of the filament lined up along the line of sight like a “cigar”. It is needed to note that the considered filament is a very small structure in comparison with the huge filaments such as the Perseus-Pisces filament (Wegner et al. 1993) or the Norma-Pavo-Indus filament (Courtois et al. 2013). The two nearest clusters of galaxies to the Sculptor Filament are the Virgo and Fornax clusters (see Fig. 1).

It was also recognized that the near and the far parts of the “cigar” are not gravitationally bound of each other and follow linear (Hubble-Lemaître) velocity-distance relation.

List with the main members of the Sculptor Filament is presented in Table 1. The object names correspond to the ones given in the Database on the Local Volume Galaxies³ (Kaisina et al. 2012). The coordinates in the table are equatorial (J 2000.0). The mass M_\star is the total stellar mass obtained from the galaxy luminosity in K -band, L_K , assuming a ratio of $M_\star/L_K \simeq 1 M_\odot/L_\odot$ (Bell et al. 2003). The radial velocity V_{LG} and the distance R are also given in Table 1. The last column contains the method used to measure the galaxy distance: the tip of red giant branch (TRGB), the Tully-Fisher relation (TF), the numerical action method (NAM). The data are available in the Database on the Local Volume Galaxies and also published in Karachentsev et al. (2013, 2014, 2017); Westmeier et al. (2017).

³<http://www.sao.ru/lv/lvddb>

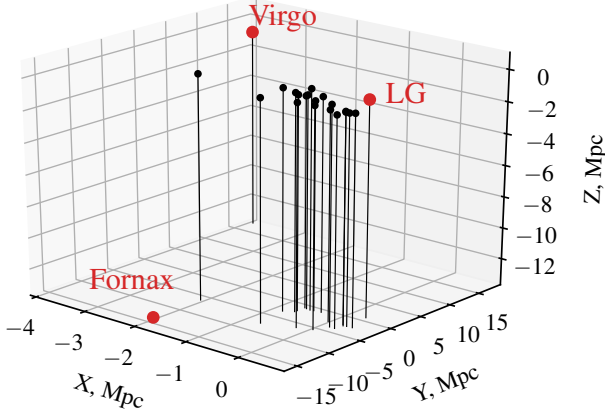


Fig. 1 Positions of the Sculptor Filament and the nearby Virgo and Fornax clusters in Cartesian Supergalactic coordinates.

Table 1 Galaxies in the Sculptor Filament and around it (N=31)

Name	Coord. RA, Dec	$\log_{10} M_*$ M_\odot	V_{LG} km s^{-1}	R Mpc	meth
ESO409-015	00 05 31.8 -28 05 53	8.10	769	8.71	TRGB
ESO349-031	00 08 13.3 -34 34 42	7.12	230	3.21	TRGB
NGC0024	00 09 56.4 -24 57 48	9.48	606	7.31	TRGB
NGC0045	00 14 03.9 -23 10 56	9.33	528	6.64	TRGB
NGC0055	00 15 08.5 -39 13 13	9.48	111	2.11	TRGB
NGC0059	00 15 25.1 -21 26 38	8.66	431	4.90	TRGB
ESO410-005	00 15 31.4 -32 10 48	6.89	53	1.93	TRGB
LV J0015-3825	00 15 38.3 -38 25 41	6.68	592	7.31	NAM
Sc22	00 23 51.7 -24 42 18	7.15	-	4.29	TRGB
ESO294-010	00 26 33.3 -41 51 20	6.30	71	2.03	TRGB
ESO473-024	00 31 22.5 -22 45 57	7.72	584	9.90	TF
ScuSR	00 33 51.8 -27 50 24	6.36	-	4.00	mem
DDO226	00 43 03.8 -22 15 01	7.71	409	4.92	TRGB
NGC0247	00 47 08.3 -20 45 36	9.50	216	3.72	TRGB
NGC0253	00 47 34.3 -25 17 32	10.98	276	3.70	TRGB
ScI-MM-Dw1	00 47 34.9 -26 23 20	6.77	-	3.94	TRGB
KDG002	00 49 21.1 -18 04 28	6.85	290	3.56	TRGB
DDO006	00 49 49.3 -21 00 58	7.08	344	3.44	TRGB
ScI-MM-Dw2	00 50 17.1 -24 44 59	7.36	-	3.12	TRGB
ESO540-032	00 50 24.6 -19 54 25	6.83	285	3.63	TRGB
NGC0300	00 54 53.5 -37 40 57	9.41	116	2.09	TRGB
LV J0055-2310	00 55 01.0 -23 10 09	6.17	288	3.70	mem
UGCA438	23 26 27.5 -32 23 26	7.59	99	2.22	TRGB
ESO347-017	23 26 56.1 -37 20 49	8.17	701	7.60	TF
IC5332	23 34 27.5 -36 06 06	9.62	716	7.80	mem
LV J2335-3713	23 35 04.1 -37 13 14	7.38	623	7.59	TRGB
NGC7713	23 36 15.0 -37 56 20	9.43	696	7.80	TF
PGC680341	23 41 47.5 -33 08 41	7.15	486	6.08	NAM
UGCA442	23 43 46.0 -31 57 33	8.03	300	4.37	TRGB
NGC7793	23 57 49.4 -32 35 24	9.70	250	3.63	TRGB
PGC704814	23 58 40.7 -31 28 03	6.90	299	3.60	mem

4 Λ N-body model

4.1 Equations of motion

Following the same logic as in Chernin et al. (2015), in our Λ N-body model, the galaxies in Sculptor Filament (with and without the Virgo and Fornax clusters) are treated as a non-relativistic isolated conservative system of point-like masses interacting with each other via Newton's mutual gravity and undergoing Einstein's antigravity produced by the dark energy background. The equations of motion for the system can be written in the following form:

$$\frac{d^2 x_i}{dt^2} = G \sum_{j=1, j \neq i}^N m_j \frac{x_j - x_i}{r_{ij}^3} + H_\Lambda^2 x_i \quad (11)$$

$$\frac{d^2 y_i}{dt^2} = G \sum_{j=1, j \neq i}^N m_j \frac{y_j - y_i}{r_{ij}^3} + H_\Lambda^2 y_i \quad (12)$$

$$\frac{d^2 z_i}{dt^2} = G \sum_{j=1, j \neq i}^N m_j \frac{z_j - z_i}{r_{ij}^3} + H_\Lambda^2 z_i \quad (13)$$

$$r_{ij} = \sqrt{(x_j - x_i)^2 + (y_j - y_i)^2 + (z_j - z_i)^2} \quad (14)$$

To work with more homogeneous set of the data for our modelling we used only the members of the Sculptor Filament with known velocities and the TRGB distances, i.e. 19 galaxies (see Table 1). We performed the calculations in the supergalactic (X, Y, Z) coordinate system. The Local Group with the Milky Way and the Andromeda galaxies is considered as one point-like source with the total mass $M = 3.11 \times 10^{12} M_\odot$. The total mass of other galaxies is estimated from the stellar mass with use of the relation $\log_{10}(M_{tot}/M_*) = \log_{10}(32) - 0.50 \times \log_{10}(M_*/10^{10})$, when $\log_{10}(M_*) < 10$ (Kourkchi and Tully 2017). The total mass for NGC0253 is adopted to $1.51 \times 10^{12} M_\odot$ (Chernin et al. 2015). Our main model includes the Virgo and Fornax clusters since they are located at the opposite sides of the filament and can potentially affect the flow. We also performed the simulations without these clusters. Their radial velocities are taken equal to 975 and 1410 km s^{-1} , the total masses — to 8×10^{14} and $1 \times 10^{14} M_\odot$, and the distances — to 17 and 20 Mpc, respectively (Karachentsev and Nasonova 2010).

We do not consider the origin and early evolution of the filament in the past. We use the observed velocities and distances of the galaxies at the present moment of

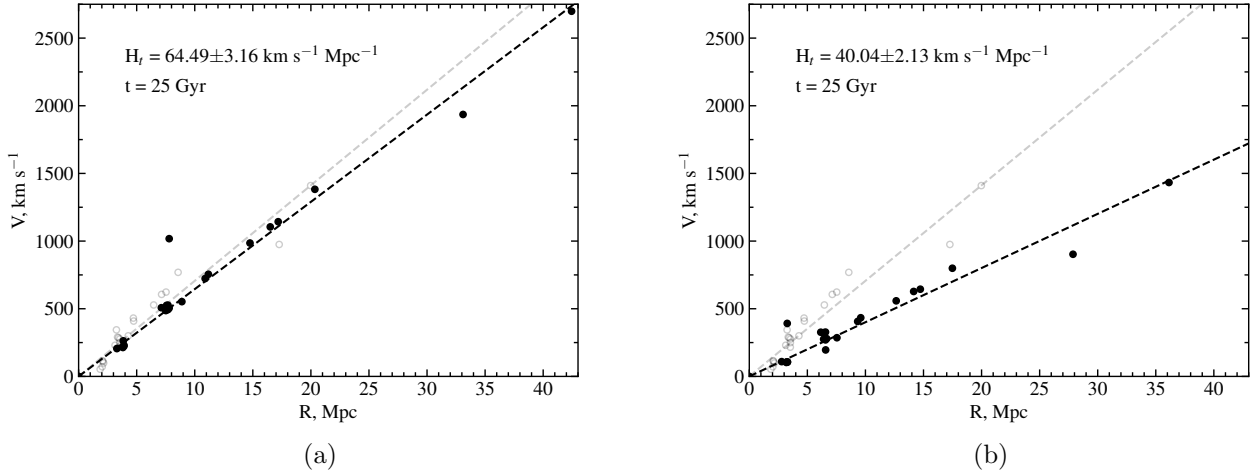


Fig. 2 Velocity-distance diagrams for the Sculptor Filament and the Virgo and Fornax clusters with (a) and without (b) dark energy term in the equations of motions for $t = 25$ Gyr. The dashed line is the fit by linear relation $V = H_t R$. The Hubble diagram based on the velocity and distance measurements in the current epoch ($t = 13.8$ Gyr) is shown by light-grey colour in both plots.

cosmic time $t = t_0 = 13.8$ Gyr (Planck Collaboration et al. 2016) as initial conditions in our model. They are listed in Table 1. Our model covers the time interval from t_0 to $t = 25$ Gyr.

The universal time-rate $H_\Lambda = \left(\frac{8\pi}{3}G\rho_\Lambda\right)^{1/2}$ is adopted to be $61 \text{ km s}^{-1} \text{ Mpc}^{-1}$. This time-rate is constant and depends on the dark energy density only (see Chernin et al. 2015 for details).

It should be noted that the tangential (transverse) velocities of the galaxies are unknown and we allow these to be zero in the initial conditions for the model⁴. Non-zero transverse velocities might change the trajectories of the flow in some way. However, they could hardly alternate the main trends of the system evolution and especially the asymptotic state of the flow because the tangential velocities vanish with the growth of the distances.

4.2 System dynamics and evolution

In Fig. 2 we compare two Hubble diagrams, with and without dark energy term in equations (11–14), at the moment $t = 25$ Gyr. For this figure, the radial distances and velocities are re-calculated to the reference frame of the Local Group barycentre. The initial positions of

galaxies are shown by light-grey colour in both plots, the final positions are coloured in black. If we take into account the dark energy term, in the end of calculations the trajectories converge to the straight line with $H_t = 64.49 \pm 3.16 \text{ km s}^{-1} \text{ Mpc}^{-1}$. This value is not very far from the present value of the time-dependent cosmological time-rate $H_0 = 67.8 \pm 0.9 \text{ km s}^{-1} \text{ Mpc}^{-1}$ found by Planck (Planck Collaboration et al. 2016). On the contrary, without dark energy $H_t \simeq 40 \text{ km s}^{-1} \text{ Mpc}^{-1}$ which does not match the current measurements. If we do not take into account the Virgo and Fornax clusters, the H_t parameter equals to $\sim 67 \text{ km s}^{-1} \text{ Mpc}^{-1}$ (with dark energy term) and $\sim 42 \text{ km s}^{-1} \text{ Mpc}^{-1}$ (without dark energy term).

It can be also noted that the length of the phase trajectories is shorter for the bodies with lower initial velocities and longer for the high-velocity galaxies. The initially slowest galaxy — ESO410 — increases its distance from 1.9 to 3.3 Mpc (1.74 times) during this time interval. The fastest galaxy — ESO409 — increases its distance from 8.7 to 20.3 Mpc (2.33 times).

As we can see from Fig. 2 the radial velocity dispersion for the outer part of the filament at the moment $t = 25$ Gyr is smaller than at the present moment which means that the flow there becomes increasingly regular and cold. However, the inner part of the filament keeps its dispersion and does not follow the global expansion caused by dark energy.

The ΛN -body model gives the spatial trajectories of galaxies in the Sculptor Filament (see their projections to the XY supergalactic plane for our main model and the model that does not include the Virgo and Fornax

⁴The Gaia end-of-mission proper motions will be able to significantly detect the mass distribution of large-scale structure on length scales < 25 Mpc which in turn will help us to determine the transverse peculiar velocities of galaxies and to improve our model in further studies (Truebenbach and Darling 2018, see also Shaya et al. 2017).

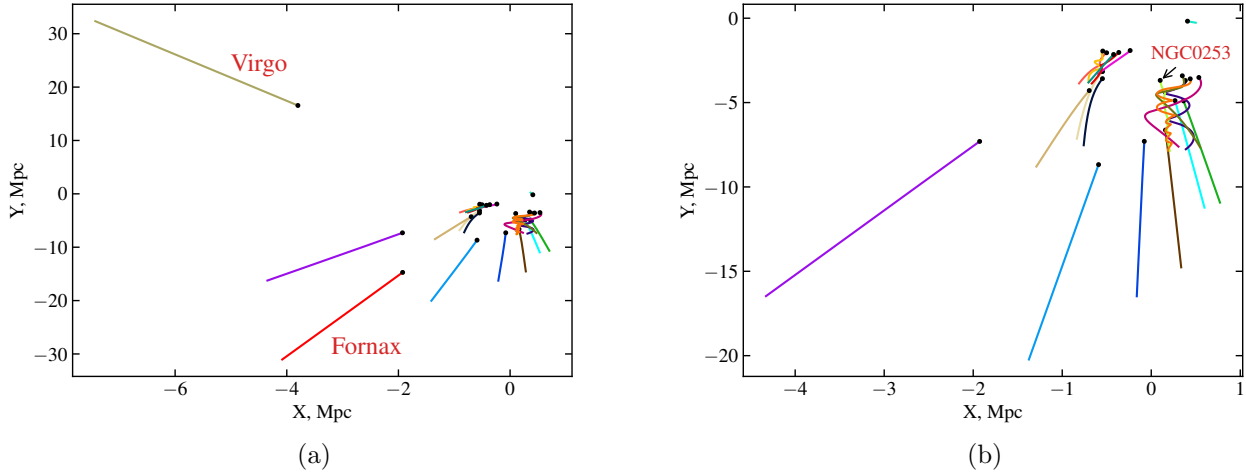


Fig. 3 Spatial trajectories of the Sculptor Filament in the projection to the XY supergalactic plane with (a) and without (b) the Virgo and Fornax clusters. Black dots denote the present-day values.

clusters in Fig. 3). In the figure we denote NGC0253, which is the most massive object in the filament after the MW-Andromeda system. In general, the distances of the bodies are increasing during the whole time of computation, and the mutual distances between them are also increasing. However, around NGC0253 the trajectories do not look like straight lines and affected by its gravity. Apparently, in this region the system experiences the multiple mutual passages and the point-like approximation does not work here. This explains the dispersion we observe for the inner part of the filament in Fig. 2.

4.3 Acceleration

The dimensionless deceleration parameter is defined as

$$q(t) = -\frac{\ddot{a}a}{\dot{a}^2}, \quad (15)$$

where $a(t)$ is the cosmological scale factor. The cosmological deceleration parameter is positive for gravity-dominated Universe and negative for antigravity-dominated Universe tending to $q(t)_\infty = -1$ in the limit of infinite cosmological expansion. At the present epoch, the cosmological deceleration parameter $q_0 \simeq -0.54$ (Planck Collaboration et al. 2016).

Let us introduce the deceleration parameter $q(R)$ as a function of the radial distance R for the galaxies in the Sculptor Filament (Chernin and Teerikorpi 2013):

$$q(t) = -\frac{\ddot{R}R}{\dot{R}^2}. \quad (16)$$

The result for both models is presented in Fig. 4 where the present-day values of the parameter are shown by black dots. It is seen from the figure that the deceleration parameter $q(R)$ is negative for each of the galaxies at all the distances and time moments under consideration. This indicates that the outer part of the Sculptor Filament is accelerating and the dark energy dominates its dynamics since the present epoch at least. We can also see that at larger distances when the mutual gravity vanished the trajectories tend to the asymptotic value $q(R)_\infty = -1$. This local asymptotic value is the same as the cosmological one $q(t)_\infty$.

5 Conclusions

Dark energy was first observed with the Hubble Space Telescope at the global cosmological distances ~ 1000 Mpc (Riess et al. 1998; Perlmutter et al. 1999). The results have later been confirmed (and refined) in the space investigations with the WMAP (Hinshaw et al. 2013) and Planck (Planck Collaboration et al. 2016) missions. Dark energy manifests itself only by its anti-gravity. This new force of nature was predicted theoretically by Einstein more than a hundred years ago. In his General Relativity equations of 1917, anti-gravity is represented by the cosmological constant Λ . A possible existence in nature of Einstein's anti-gravity was taken into account in Friedmann's global cosmological theory; the cosmological constant is an empirical parameter that should be measured in astronomical observations. General Relativity indicates that dark energy exists not only in the space of the global Universe, where it was first observed, but actually everywhere in

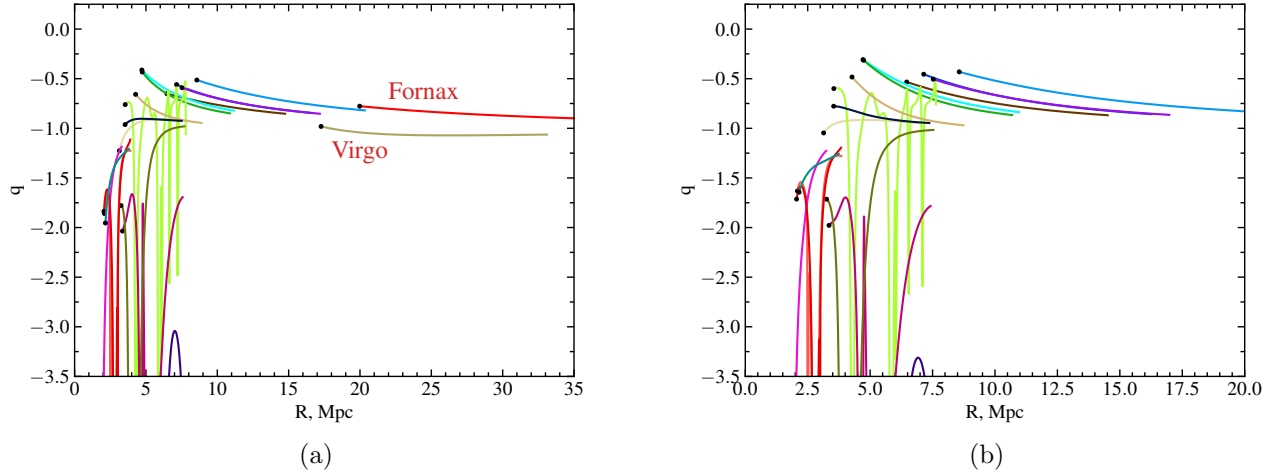


Fig. 4 Deceleration parameter $q(R)$ as a function of the radial distance of the Sculptor Filament with (a) and without (b) the Virgo and Fornax clusters. Black dots denote the present-day values.

the physical space, including the local distances of 1–30 Mpc where the distribution of galaxies is, generally, non-uniform. Since Friedmann’s theory does not work there, a theory that would take into account the really observed distribution of galaxies in different space volumes is needed.

The building blocks of the Cosmic Web are 3D groups and clusters of galaxies, 2D walls like the Local Supercluster and 1D filaments. These systems are observed on both global and local spatial scales. All of them are embedded in the omnipresent dark energy background. We studied the nearest 3D expansion flows around the groups (the Local Group and several similar groups) and the Coma and Virgo clusters (Chernin 2001, 2008, 2013); 2D Zel’dovich Local Pancake (Chernin et al. 2015). The HST recent accurate data on these systems are provided by Karachentsev and his co-workers (Karachentsev et al. 2003, 2013). In this work the N-body model for 1D Sculptor Filament of galaxies has been constructed. We performed the calculations in two versions. The main model included the influence of the Virgo and Fornax clusters. In the other version, only the filament members were considered. We showed that the dark energy domination in the Sculptor Filament is not strongly affected by the most massive nearby clusters of galaxies. However, their gravity slightly modifies the spatial trajectories of the filament members. Both computer models demonstrated that the motions of outer parts of the filament are driven by the dark energy while the mutual gravity of the bodies is relatively weak. On the contrary the inner part is subjected to the mutual gravity and point-like approximation does not work for it. Therefore, the outer part of the filament as well as 2D and 3D systems

reveal a common feature: in all the systems, the dark energy anti-gravity is stronger than the self gravity of the galaxies. Because of this, the objects in the Sculptor Filament expand with acceleration tending with time to the linear velocity-distance relation with H_0 value close to the current one.

6 Compliance with Ethical Standards

The manuscript complies to the Ethical Rules of Astrophysics and Space Science. There are no any conflicts of interest.

Acknowledgements

We are grateful to N. V. Emelyanov, Yu. N. Efremov, G. S. Bisnovatyi-Kogan, and A. V. Zasov for helpful discussions. M.V.P. acknowledges support from Russian Science Foundation grant 18-72-00159 for the Hubble diagram analysis and Lomonosov Moscow State University Program of Development “Leading Science Schools of MSU: Physics of Stars, Relativistic Compact Objects and Galaxies” for the Λ N-body simulations.

References

- V. A. Ambartsumian. On the Evolution of Galaxies. *Izvestiya Akademii Nauk Armianskoi*, 11:9–37, January 1958a.
- V. A. Ambartsumian. On the Problem of the Mechanism of the Origin of Stars in Stellar Associations. *Reviews of Modern Physics*, 30(3):944–948, July 1958b. doi: 10.1103/RevModPhys.30.944.
- V. A. Ambartsumyan. Problems of Extragalactic Research. *Problems of Cosmogeny*, 8:2, January 1962.
- H. Arp. HI clouds in the Sculptor and local groups. *Astron. J.*, 90:1012–1018, June 1985. doi: 10.1086/113808.
- Eric F. Bell, Daniel H. McIntosh, Neal Katz, and Martin D. Weinberg. The Optical and Near-Infrared Properties of Galaxies. I. Luminosity and Stellar Mass Functions. *Astrophys. J. Suppl. Ser.*, 149(2):289–312, December 2003. doi: 10.1086/378847.
- A. D. Chernin. Clusters of galaxies and the cosmological expansion. In S. N. Vernov and G. E. Kocharov, editors, *Sixth Winter School on Space Physics*, page 37, January 1971.
- A. D. Chernin. REVIEWS OF TOPICAL PROBLEMS: Cosmic vacuum. *Physics Uspekhi*, 44:1099–1118, November 2001. doi: 10.1070/PU2001v044n11ABEH000962.
- A. D. Chernin. PHYSICS OF OUR DAYS: Dark energy and universal antigravitation. *Physics Uspekhi*, 51:253–282, March 2008. doi: 10.1070/PU2008v051n03ABEH006320.
- A. D. Chernin. Dark energy in systems of galaxies. *Soviet Journal of Experimental and Theoretical Physics Letters*, 98:353–364, November 2013. doi: 10.1134/S002136401319003X.
- A. D. Chernin. Gravity-antigravity interplay in the local galaxy flows. *Baltic Astronomy*, 25:296–299, Jan 2016. doi: 10.1515/astro-2017-0133.
- A. D. Chernin and P. Teerikorpi. Local expansion flows of galaxies: quantifying acceleration effect of dark energy. *Astronomical and Astrophysical Transactions*, 28: 177–184, August 2013.
- A. D. Chernin, I. D. Karachentsev, O. G. Nasonova, P. Teerikorpi, M. J. Valtonen, V. P. Dolgachev, L. M. Domozhilova, and G. G. Byrd. Dark energy domination in the Virgocentric flow. *Astron. Astrophys.*, 520:A104, September 2010. doi: 10.1051/0004-6361/201014912.
- A. D. Chernin, N. V. Emelyanov, and I. D. Karachentsev. Dark energy domination in the local flow of giant galaxies. *Mon. Not. R. Astron. Soc.*, 449:2069–2078, May 2015. doi: 10.1093/mnras/stv144.
- Hélène M. Courtois, Daniel Pomarède, R. Brent Tully, Yehuda Hoffman, and Denis Courtois. Cosmography of the Local Universe. *Astron. J.*, 146(3):69, September 2013. doi: 10.1088/0004-6256/146/3/69.
- G. de Vaucouleurs. An Expanding Association of Galaxies. *Astrophys. J.*, 130:718, November 1959. doi: 10.1086/146763.
- Wendy L. Freedman, Barry F. Madore, Dylan Hatt, Taylor J. Hoyt, In Sung Jang, Rachael L. Beaton, Christopher R. Burns, Myung Gyoong Lee, Andrew J. Monson, Jillian R. Neeley, M. M. Phillips, Jeffrey A. Rich, and Mark Seibert. The Carnegie-Chicago Hubble Program. VIII. An Independent Determination of the Hubble Constant Based on the Tip of the Red Giant Branch. *Astrophys. J.*, 882(1):34, Sep 2019. doi: 10.3847/1538-4357/ab2f73.
- E. B. Gliner. Algebraic Properties of the Energy-momentum Tensor and Vacuum-like States of o^+ Matter. *Soviet Journal of Experimental and Theoretical Physics*, 22:378, February 1966.
- G. Hinshaw, D. Larson, E. Komatsu, D. N. Spergel, C. L. Bennett, J. Dunkley, M. R. Nolte, M. Halpern, R. S. Hill, N. Odegard, L. Page, K. M. Smith, J. L. Weiland, B. Gold, N. Jarosik, A. Kogut, M. Limon, S. S. Meyer, G. S. Tucker, E. Wollack, and E. L. Wright. Nine-year Wilkinson Microwave Anisotropy Probe (WMAP) Observations: Cosmological Parameter Results. *Astrophys. J. Suppl. Ser.*, 208:19, October 2013. doi: 10.1088/0067-0049/208/2/19.
- E. Hubble. A Relation between Distance and Radial Velocity among Extra-Galactic Nebulae. *Proceedings of the National Academy of Science*, 15:168–173, March 1929. doi: 10.1073/pnas.15.3.168.
- H. Jerjen, K. C. Freeman, and B. Binggeli. Surface Brightness Fluctuation Distances to Dwarf Elliptical Galaxies in the Sculptor Group. *Astron. J.*, 116:2873–2885, December 1998. doi: 10.1086/300635.
- E. I. Kaisina, D. I. Makarov, I. D. Karachentsev, and S. S. Kaisin. Observational database for studies of nearby universe. *Astrophysical Bulletin*, 67(1):115–122, January 2012. doi: 10.1134/S1990341312010105.
- I. D. Karachentsev and O. G. Nasonova. The observed infall of galaxies towards the Virgo cluster. *Mon. Not. R. Astron. Soc.*, 405:1075–1083, June 2010. doi: 10.1111/j.1365-2966.2010.16501.x.
- I. D. Karachentsev, E. K. Grebel, M. E. Sharina, A. E. Dolphin, D. Geisler, P. Guhathakurta, P. W. Hodge, V. E. Karachentseva, A. Sarajedini, and P. Seitzer. Distances to nearby galaxies in Sculptor. *Astron. Astrophys.*, 404: 93–111, June 2003. doi: 10.1051/0004-6361:20030170.
- I. D. Karachentsev, V. E. Karachentseva, W. K. Huchtmeier, and D. I. Makarov. A Catalog of Neighboring Galaxies. *Astron. J.*, 127:2031–2068, April 2004. doi: 10.1086/382905.
- I. D. Karachentsev, E. I. Kaisina, and D. I. Makarov. Suites of Dwarfs around nearby Giant Galaxies. *Astron. J.*, 147: 13, January 2014. doi: 10.1088/0004-6256/147/1/13.
- Igor D. Karachentsev, Dmitry I. Makarov, and Elena I. Kaisina. Updated Nearby Galaxy Catalog. *Astron. J.*, 145 (4):101, April 2013. doi: 10.1088/0004-6256/145/4/101.
- Igor D. Karachentsev, Elena I. Kaisina, and Olga G. Kashibadze “Nasonova”. The Local Tully-Fisher Relation for Dwarf Galaxies. *Astron. J.*, 153(1):6, January 2017. doi: 10.3847/1538-3881/153/1/6.
- Ehsan Kourkchi and R. Brent Tully. Galaxy Groups Within 3500 km s⁻¹. *Astrophys. J.*, 843(1):16, Jul 2017. doi: 10.3847/1538-4357/aa76db.
- G. Lemaître. Un Univers homogène de masse constante et de rayon croissant rendant compte de la vitesse radiale des nébuleuses extra-galactiques. *Annales de la Société Scientifique de Bruxelles*, 47:49–59, 1927.

- S. Perlmutter, G. Aldering, G. Goldhaber, R. A. Knop, P. Nugent, P. G. Castro, S. Deustua, S. Fabbro, A. Goobar, D. E. Groom, I. M. Hook, A. G. Kim, M. Y. Kim, J. C. Lee, N. J. Nunes, R. Pain, C. R. Penny-
packer, R. Quimby, C. Lidman, R. S. Ellis, M. Irwin, R. G. McMahon, P. Ruiz-Lapuente, N. Walton, B. Schaefer, B. J. Boyle, A. V. Filippenko, T. Matheson, A. S. Fruchter, N. Panagia, H. J. M. Newberg, W. J. Couch, and T. S. C. Project. Measurements of Ω and Λ from 42 High-Redshift Supernovae. *Astrophys. J.*, 517:565–586, June 1999. doi: 10.1086/307221.
- Planck Collaboration, P. A. R. Ade, N. Aghanim, M. Arnaud, M. Ashdown, J. Aumont, C. Baccigalupi, A. J. Banday, R. B. Barreiro, J. G. Bartlett, and et al. Planck 2015 results. XIII. Cosmological parameters. *Astron. Astrophys.*, 594:A13, September 2016. doi: 10.1051/0004-6361/201525830.
- Planck Collaboration, N. Aghanim, Y. Akrami, M. Ashdown, J. Aumont, C. Baccigalupi, and et al. Planck 2018 results. VI. Cosmological parameters. *arXiv e-prints*, art. arXiv:1807.06209, Jul 2018.
- A. G. Riess, A. V. Filippenko, P. Challis, A. Clocchiatti, A. Diercks, P. M. Garnavich, R. L. Gilliland, C. J. Hogan, S. Jha, R. P. Kirshner, B. Leibundgut, M. M. Phillips, D. Reiss, B. P. Schmidt, R. A. Schommer, R. C. Smith, J. Spyromilio, C. Stubbs, N. B. Suntzeff, and J. Tonry. Observational Evidence from Supernovae for an Accelerating Universe and a Cosmological Constant. *Astron. J.*, 116:1009–1038, September 1998. doi: 10.1086/300499.
- Adam G. Riess, Stefano Casertano, Wenlong Yuan, Lucas M. Macri, and Dan Scolnic. Large Magellanic Cloud Cepheid Standards Provide a 1% Foundation for the Determination of the Hubble Constant and Stronger Evidence for Physics beyond Λ CDM. *Astrophys. J.*, 876(1): 85, May 2019. doi: 10.3847/1538-4357/ab1422.
- H.P. Robertson. On relativistic cosmology. *Philosophical Magazine*, 5:835–848, 1928.
- D. M. Scolnic, D. O. Jones, A. Rest, Y. C. Pan, R. Chornock, and et al. The Complete Light-curve Sample of Spectroscopically Confirmed SNe Ia from Pan-STARRS1 and Cosmological Constraints from the Combined Pantheon Sample. *Astrophys. J.*, 859:101, June 2018. doi: 10.3847/1538-4357/aab9bb.
- Edward J. Shaya, R. Brent Tully, Yehuda Hoffman, and Daniel Pomarède. Action Dynamics of the Local Supercluster. *Astrophys. J.*, 850(2):207, December 2017. doi: 10.3847/1538-4357/aa9525.
- E. Tempel, R. S. Stoica, V. J. Martínez, L. J. Liivamägi, G. Castellan, and E. Saar. Detecting filamentary pattern in the cosmic web: a catalogue of filaments for the SDSS. *Mon. Not. R. Astron. Soc.*, 438:3465–3482, March 2014. doi: 10.1093/mnras/stt2454.
- Alexandra E. Truebenbach and Jeremy Darling. Toward a Measurement of the Transverse Peculiar Velocity of Galaxy Pairs. *Astrophys. J.*, 868(1):69, November 2018. doi: 10.3847/1538-4357/aae830.
- Gary Wegner, Martha P. Haynes, and Riccardo Giovanelli. A Survey of the Pisces-Perseus. V. The Declination Strip +33.5 degrees to +39.5 degrees and the Main Supercluster Ridge. *Astron. J.*, 105:1251, April 1993. doi: 10.1086/116507.
- T. Westmeier, D. Obreschkow, M. Calabretta, R. Jurek, B. S. Koribalski, M. Meyer, A. Musaeva, A. Popping, L. Staveley-Smith, O. I. Wong, and A. Wright. A deep Parkes H I survey of the Sculptor group and filament: H I mass function and environment. *Mon. Not. R. Astron. Soc.*, 472(4):4832–4850, December 2017. doi: 10.1093/mnras/stx2289.